The Plant Cell, Vol. 25: 3699–3710, October 2013, www.plantcell.org

LARGE-SCALE BIOLOGY ARTICLE

Translational Landscape of Photomorphogenic *Arabidopsis*[W]

Ming-Jung Liu,[a,1] Szu-Hsien Wu,[a,b,c] Jing-Fen Wu,[a] Wen-Dar Lin,[a] Yi-Chen Wu,[a] Tsung-Ying Tsai,[a] Huang-Lung Tsai,[a] and Shu-Hsing Wu[a,b,c,2]

[a] Institute of Plant and Microbial Biology, Academia Sinica, Taipei 11529, Taiwan
[b] Molecular and Biological Agricultural Sciences Program, Taiwan International Graduate Program, Academia Sinica, Taipei 11529, Taiwan
[c] Graduate Institute of Biotechnology and Department of Life Sciences, National Chung-Hsing University, Taichung 402, Taiwan

ORCID ID: 0000-0002-7179-3138 (Sh.-H.-W.).

Translational control plays a vital role in regulating gene expression. To decipher the molecular basis of translational regulation in photomorphogenic *Arabidopsis thaliana*, we adopted a ribosome profiling method to map the genome-wide positions of translating ribosomes in *Arabidopsis* etiolated seedlings in the dark and after light exposure. We found that, in *Arabidopsis*, a translating ribosome protects an ~30-nucleotide region and moves in three-nucleotide periodicity, characteristics also observed in *Saccharomyces cerevisiae* and mammals. Light enhanced the translation of genes involved in the organization and function of chloroplasts. Upstream open reading frames initiated by ATG but not CTG mediated translational repression of the downstream main open reading frame. Also, we observed widespread translational repression of microRNA target genes in both light- and dark-grown *Arabidopsis* seedlings. This genome-wide characterization of transcripts undergoing translation at the nucleotide-resolution level reveals that a combination of multiple translational mechanisms orchestrates and fine-tunes the translation of diverse transcripts in plants with environmental responsiveness.

INTRODUCTION

Gene expression involves producing RNA and/or protein products from genetic codes. However, whole-genome proteomic profiling remains a challenge compared with transcriptomic profiling, which has been promoted by technical advances such as microarray and next-generation sequencing.

The association of transcripts with polysomes implies their active translation status. Microarray profiling of mRNAs associated with polysomes has provided fundamental information for identifying transcripts undergoing translation (Melamed and Arava, 2007; Mustroph et al., 2009). With this methodology, differential translations of mRNA populations were observed in the model plant *Arabidopsis thaliana* responding to various external stimuli, including dehydration, elevated temperature, high salinity, oxygen deprivation, Suc starvation, and heavy metal, light, and gibberellin treatment (Kawaguchi et al., 2004; Branco-Price et al., 2005, 2008; Nicolaï et al., 2006; Matsuura et al., 2010; Sormani et al., 2011; Liu et al., 2012; Ribeiro et al., 2012). However, this approach simply measures the existence and abundance of polysome-associated transcripts; it does not offer the resolution to reveal which part of the transcript is being translated, which is especially important given the multiple in-frame start codons or separate translation units that are commonly present in eukaryotic transcripts. Indeed, several studies have demonstrated that translational regulation could occur at various levels. These include alternative translation initiation with one transcript producing two proteins targeted to different organelles, microRNA (miRNA)–mediated repression of translation by pausing ribosomes or accelerating ribosome drop-off, and lower reinitiation efficiency of main open reading frames (mORFs) by the translation of upstream open reading frames (uORFs) in the 5′ untranslated region (UTR) (reviewed in Morris and Geballe, 2000; Mackenzie, 2005; Fabian et al., 2010; Huntzinger and Izaurralde, 2011). To fully understand translational regulation, we need to measure the dynamic positional information and abundance of translating ribosomes on a transcript. Information about the translation landscape also offers knowledge on how an organism could use translational regulation to cope with the internal developmental program and respond to external environmental stimuli.

Ribosome profiling, combining RNase protection assays with deep sequencing, has allowed for comprehensive and precise mapping of the positions of translating ribosomes on transcripts (Ingolia et al., 2009). Studies of yeast (*Saccharomyces cerevisiae*) and mammals have revealed sequence features associated with translational regulation under various conditions (Ingolia et al., 2009; Guo et al., 2010; Ingolia et al., 2011; Brar et al., 2012). However, a genome-wide map of active translation in plants has not been reported.

In *Arabidopsis*, the profiling of mRNAs associated with polysomes has revealed transcripts with translation regulated by environmental light signals (Piques et al., 2009; Juntawong and Bailey-Serres, 2012; Liu et al., 2012). In this study, we used ribosome profiling to build a high-resolution translational map of

[1] Current address: Department of Plant Biology, Michigan State University, East Lansing, MI 48824.
[2] Address correspondence to shuwu@gate.sinica.edu.tw.
The author responsible for distribution of materials integral to the findings presented in this article in accordance with the policy described in the Instructions for Authors (www.plantcell.org) is: Shu-Hsing Wu (shuwu@gate.sinica.edu.tw).
[W] Online version contains Web-only data.
www.plantcell.org/cgi/doi/10.1105/tpc.113.114769

transcripts in *Arabidopsis* seedlings undergoing photomorphogenic development. We assessed how external light signals coordinate with internal *cis*-sequence features to regulate the translation of expressed genes in *Arabidopsis*.

RESULTS

Monitoring Translation with Single-Nucleotide Resolution in Photomorphogenic *Arabidopsis*

We used ribosome profiling to monitor dynamic translational changes in *Arabidopsis* undergoing photomorphogenic development, when a dark-grown seedling first senses light signals (Figure 1A). *Arabidopsis* 4-d-old etiolated seedlings were exposed to light, and the aerial parts were harvested at 0 min (dark) and after 4-h light (L4h). RNA gel blot analysis revealed that ribosome-protected fragments (RPFs; $mRNA_{RP}$) in *Arabidopsis* were ~30 nucleotides (see Supplemental Figure 1 online), similar to that in yeast and mammals (Ingolia et al., 2009; Guo et al., 2010).

We obtained ~5 and ~40 million unique mapped reads for $mRNA_{RP}$ and the randomly fragmented mRNA fragments (steady state mRNA [$mRNA_{SS}$]), respectively, for replicate 1 (see Supplemental Figures 2A and 2B online). Two independent biological replicates showed high data reproducibility for the 15,384 expressed genes at both $mRNA_{SS}$ and $mRNA_{RP}$ levels (R^2 = 0.8 to 0.88; Figure 1B). Despite a significant increase in $mRNA_{RP}$ reads in replicate 2 (~15 and ~41 million unique mapped reads for dark and L4h samples, respectively), similar numbers of genes with comparable read densities were identified (see Supplemental Figure 3A online). This indicated that both replicates exhausted the majority of translating mRNAs in photomorphogenic *Arabidopsis* seedlings. For most transcripts, $mRNA_{RP}$ densities (in reads per kilobase per million [RPKM]) positively correlated with the $mRNA_{SS}$ density (see Supplemental Figure 3B online) in both replicates.

The reads for $mRNA_{SS}$ were evenly distributed on UTRs and coding sequences (CDSs), but reads for $mRNA_{RP}$ were predominantly mapped to the CDS, especially surrounding the annotated initiation and stop codons (results for both biological replicates in Figure 2 and Supplemental Figure 4 online). This finding is consistent with the differential association of ribosomes with CDS (Ingolia et al., 2009, 2011; Guo et al., 2010) and supports the idea that we have obtained successful ribosome profiling results.

A translating ribosome moves three nucleotides for each translational cycle. Position analyses of aligned reads on the three nucleotides of each codon revealed a three-nucleotide periodicity for only $mRNA_{RP}$ (see Supplemental Figure 5A online) as observed in yeast and humans (Ingolia et al., 2009; Guo et al., 2010). In contrast with the higher ribosome density for the first 30 to 40 codons in yeast (Ingolia et al., 2009), ribosome density was lower in the first 30 codons with both dark and L4h treatment in *Arabidopsis* (see Supplemental Figure 5B online).

In yeast, more rare codons are found immediately after the start codon. This sequence feature leads to a lower moving speed of the translating ribosomes and a higher ribosome density in the first 30 to 50 codons, known as a ramp phenomenon

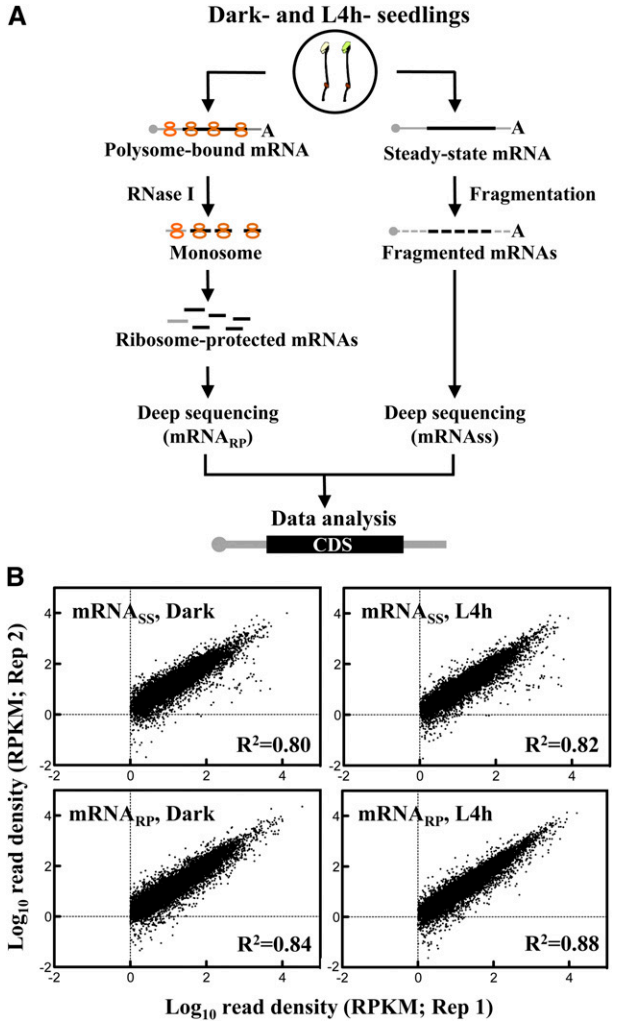

Figure 1. Profiles of Steady State and Ribosome-Protected mRNAs in Photomorphogenic *Arabidopsis*.

(A) Schematic illustration of the experimental design. $mRNA_{SS}$ and $mRNA_{RP}$ were isolated in parallel for deep sequencing of *Arabidopsis* seedlings grown in the dark or treated with white light for 4 h (L4h).
(B) High correlation of $mRNA_{SS}$ and $mRNA_{RP}$ density in dark and L4h with two biological replicates. The *x* and *y* axis show the $\log_{10}$ values of $mRNA_{SS}$ and $mRNA_{RP}$ densities (RPKMs) in CDS regions from two biological replicates of dark and L4h samples as marked.

(Tuller et al., 2010). Although a similar ramp feature was also observed for *Arabidopsis* transcripts (see Supplemental Figure 5C online), this region showed lower ribosome density (see Supplemental Figure 5B online). Similarly, the ramp feature was not associated with high ribosome density in mouse embryonic stem cells (Ingolia et al., 2011). Alternatively, the addition of the translational inhibitor cycloheximide at the time of polysome extraction may leave a time window allowing for continuing elongation of translating ribosomes.

These results suggest that the translating ribosomes in *Arabidopsis*, yeast, and mammals possess both conserved and distinct action characteristics when moving along transcripts.

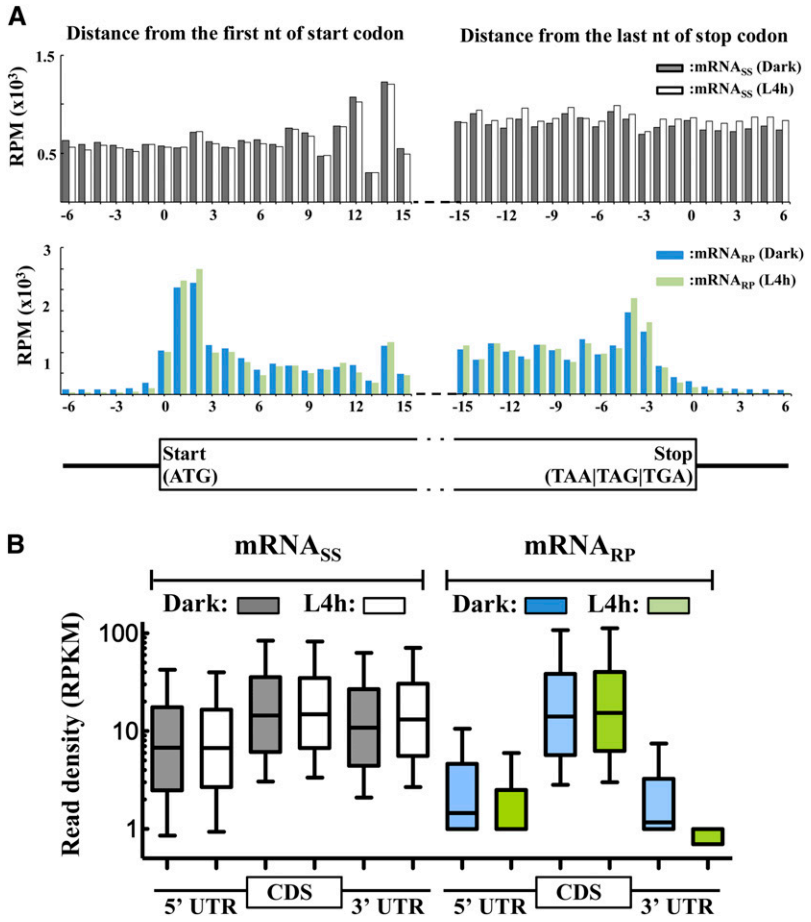

Figure 2. mRNA$_{RP}$ Reads Are Enriched in CDS.

(A) Distribution of aligned reads, in reads per million (RPM), on the annotated gene model at mRNA$_{SS}$ and mRNA$_{RP}$ levels for genes with 5′ UTR ≥ 6 nucleotides (n = 21,354) and 3′ UTR ≥ 6 nucleotides (n = 22,001). The read count for each gene was measured using the 15th nucleotide of the aligned reads.

(B) Box plots show the read density (RPKMs) for the 5′ UTRs, coding regions (CDS), and 3′ UTRs of mRNA$_{SS}$ and mRNA$_{RP}$ in the dark and L4h. Shown are expressed genes (detailed in Supplemental Figure 2A online) with UTR ≥ 1 nucleotides (n = 15,226). The top, middle, and bottom of the box represent the 25, 50, and 75 percentiles, and the top and bottom black lines are the 10th and 90th percentiles, respectively.

Light Enhances Gene Expression by Adjusting Ribosome Density

Ribosome occupancy refers to the proportion of the transcript associated with polysomes, whereas ribosome density indicates the number of ribosomes on transcripts (Arava et al., 2003; Lackner and Bähler, 2008; Piques et al., 2009). Light-regulated translation could be achieved by adjusting both the ribosome occupancy and ribosome density (Piques et al., 2009; Juntawong and Bailey-Serres, 2012; Liu et al., 2012). These previous studies mostly revealed mRNA species with significant changes in ribosome occupancy but lacked the resolution to determine the actual distribution of translating ribosomes on a given transcript. For example, steady state transcript levels and ribosome occupancy of *AT5G47110.1* and *AT4G02510.1* did not significantly differ between the dark and L4h samples in our previous study (Liu et al., 2012). However, these two transcripts were preferentially translated under light by increasing the ribosome density (mRNA$_{RP}$) (Figure 3A; see Supplemental Figure 6A online). Two transcripts, *AT3G25800.1* and *AT3G17770.1*, not regulated at the translational level are shown for comparison (Figure 3B; see Supplemental Figure 6B online).

Ribosome profiling of deetiolating *Arabidopsis* allowed us to identify genes significantly upregulated (z-score >2) or downregulated (z-score <−2) in translation in both biological replicates (Figure 3C; see Supplemental Figure 6C and Supplemental Data Set 1 online). Many of these genes were not identified in our previous study because of their comparable ribosome occupancy between dark and L4h samples (marked in red in Supplemental Data Set 1 online). Thus, ribosome profiling could effectively identify new target transcripts under translational regulation, especially those with significant changes in ribosome density. To address the functional role of these new target genes, we performed the gene ontology analyses in the category of biological

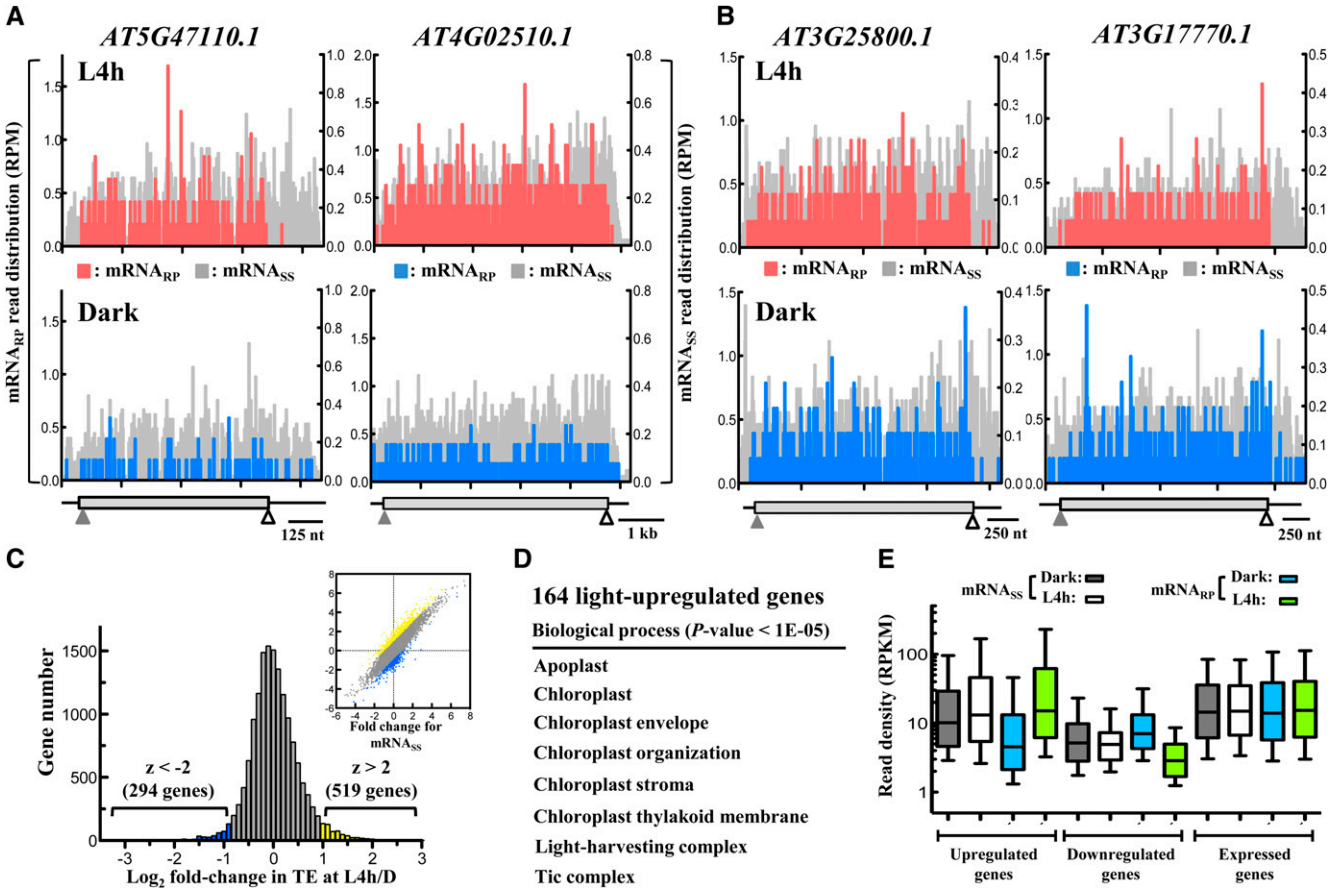

Figure 3. Ribosome Profiling Identifies Additional Genes Regulated at the Translational Level in Photomorphogenic *Arabidopsis*.

(A) and **(B)** Read distributions along the transcript at $mRNA_{SS}$ and $mRNA_{RP}$ levels were plotted for *AT5G47110.1* and *AT4G02510.1*, identified as translationally upregulated genes with light treatment **(A)** and *AT3G25800.1* and *AT3G17770.1*, identified as nontranslationally regulated genes with light treatment **(B)**. nt, nucleotides; RPM, reads per million.

(C) Distribution of changes in TE between dark and L4h samples. Yellow and blue indicate genes with expression significantly up- and downregulated, respectively, with light treatment. The $\log_2$ values of the fold changes were plotted for the defined expressed genes (n = 15,384). Bin size for fold changes in TE is 0.1.

(D) Gene ontology analysis of the biological process represented by the newly identified genes with expression significantly upregulated by light at the translational level. Only the genes identified in both biological replicates were included for the gene ontology analyses.

(E) Box plots show the $mRNA_{SS}$ or $mRNA_{RP}$ density (RPKMs) in CDS regions in the dark and L4h. Shown are expressed, upregulated, or downregulated genes in response to light. The expressed genes were defined as detailed in Supplemental Figure 2A online.

process. The newly identified genes upregulated translationally by light were mostly involved in processes related to the organization and function of chloroplasts (P value < 1E-05; Figure 3D). Our previous study showed that genes dedicated to photosynthesis were preferentially translated via increasing their ribosome occupancy (Liu et al., 2012). These results highlight that different levels of translational regulation together promote the efficient biogenesis of proteins for functional chloroplasts and photosynthesis.

In general, genes upregulated translationally had greater $mRNA_{SS}$ density than those downregulated translationally. However, the high $mRNA_{SS}$ density did not guarantee a high ribosome density ($mRNA_{RP}$) (Figure 3E; see Supplemental Figure 6D online). We observed a slight light-induced increase of $mRNA_{SS}$ density for the upregulated genes, but the increase could not account for the marked increase in $mRNA_{RP}$ density (Figure 3E; see Supplemental Figure 6D online). By contrast, genes downregulated translationally showed significantly lower $mRNA_{SS}$ density than those upregulated by light or all expressed genes. For downregulated genes, dark and L4h samples showed comparable $mRNA_{SS}$ density, but light specifically reduced their ribosome density (Figure 3E; see Supplemental Figure 6D online). These data suggested that, independent of transcript abundance, a light-dependent and selective mechanism exists for increasing or decreasing the ribosome density of specific transcripts (Figure 3E; see Supplemental Figure 6D online).

Global Identification of Expressed uORFs

Previous studies had predicted the presence of uORFs in 5′ UTRs of 20 to 60% of plant transcripts (Pesole et al., 2000; Hayden and Jorgensen, 2007; Kim et al., 2007). However, whether these annotated uORFs can engage in translation or function to regulate gene expression has not been globally studied in *Arabidopsis*. We used our ribosome profiling data to differentiate between expressed and unexpressed uORFs with ATG as an initiation codon (see Supplemental Figure 7 and Supplemental Data Set 2 online). In all, 1996 expressed genes contained 3177 expressed uORFs on their 5′ UTRs, but 3615 expressed genes contained 6927 unexpressed uORFs. $mRNA_{RP}$ density was significantly higher for the expressed uORFs than the flanking 5′ UTR sequences, but $mRNA_{SS}$ reads did not show a distribution preference (see Supplemental Figure 8A online). $mRNA_{RP}$ reads also showed a three-nucleotide periodicity associated with uORFs (see Supplemental Figure 8B online). These shared features between uORFs and the annotated open reading frames (ORFs) (Figure 2A; see Supplemental Figure 8A online) suggested that the expressed uORFs we identified were indeed under active translation in deetiolating *Arabidopsis*.

We next sought unique features associated with the translating uORFs. As compared with unexpressed uORFs, expressed uORFs were longer, more distal to the 5′ termini, and closer to the downstream annotated initiation codon ATG (Figure 4A; see Supplemental Figure 9A online). The shorter distance between the expressed uORFs and the downstream initiation codon was not due to the uORFs residing on transcripts with shorter 5′ UTRs. Rather, uORFs on transcripts with longer 5′ UTRs were more prone to be translated (Figure 4A; see Supplemental Figure 9A online).

Previous studies have shown a strong bias toward nucleotide A or G at −3 or +4 relative to translation start site, termed the Kozak sequence (Kozak, 1986, 1987a). Sequence context analysis showed that, compared with unexpressed uORFs, expressed uORFs had a significantly higher proportion of nucleotide G both in positions −3 and +4 (top panels in Figure 4B and Supplemental Figure 9B online). The expressed uORFs did not have a strong Kozak sequence context as seen for downstream mORFs (Figure 4B; see Supplemental Figure 9B online), which may reflect the regulatory nature of uORFs. Expressed uORFs and mORFs showed some differences in codon usage (Figure 4C; see Supplemental Figure 9C online; Pearson correlation r = 0.3 to 0.33), but this was largely due to the sequence

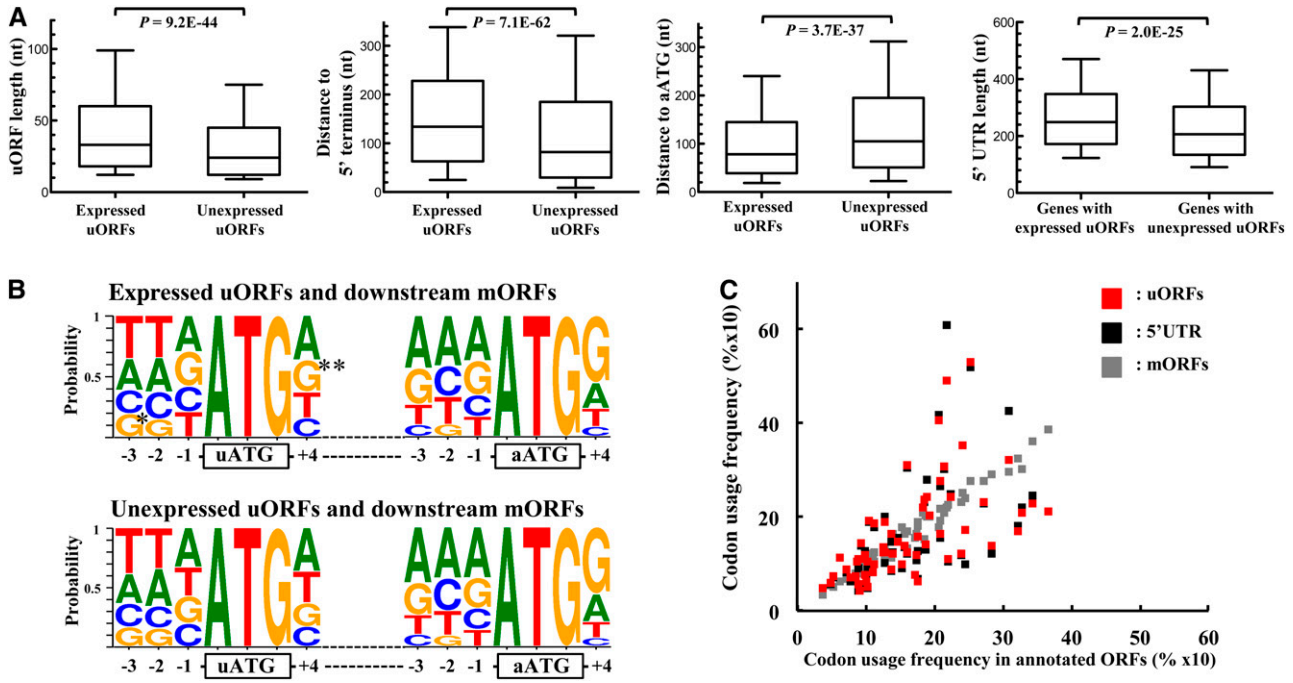

Figure 4. Sequence Characteristics of Expressed uORFs in *Arabidopsis* Transcripts.

(A) Box plots of expressed and unexpressed uORFs by mRNA features, including uORF length, distance to 5′ terminus, distance to annotated ATG, and 5′ UTR length of transcripts with uORF(s). P values were determined by Kolmogorov-Smirnov test. Data for 10th to 90th percentiles for each category are as in Figure 2. nt, nucleotides.

(B) Sequence logo results show the probability of base composition for sequence contexts of uATGs and annotated ATGs. Sequence logos for the expressed or unexpressed uORFs and their downstream mORFs are shown separately. *, G is overpresented at the −3 position (P value = 2.8E-04') **, G is overpresented at the +4 position (P value = 7.1E-15). P values were determined by one-tailed Fisher's exact test.

(C) Comparison of codon usage for annotated ORFs and 3067 expressed uORFs (red square), 1996 mORFs with expressed uORFs (gray square), or 5′ UTRs of 1996 mORFs with expressed uORFs (black square). Usage frequency of the 61 codons (excluding the three stop codons) was ranked from low to high according to usage frequency in annotated ORFs.

composition of the 5′ UTRs rather than to a selective presence of specific codons in uORFs (Figure 4C; see Supplemental Figure 9C online; Pearson correlation r = 0.96 to 0.97 for frequencies of codon usage between 5′ UTR and uORFs).

Translation of ATG-Initiated uORFs Represses the Translation of Main ORFs in a Light-Dependent Manner

In a few *Arabidopsis* genes studied, uORFs could trigger a translational repression of their downstream mORFs in response to various environmental stimuli (Hanfrey et al., 2002; Wiese et al., 2004; Nishimura et al., 2005; Imai et al., 2006; Alatorre-Cobos et al., 2012; Rosado et al., 2012). We wondered whether this function was widespread in *Arabidopsis*. Compared with transcripts with unexpressed uORFs, those with increasing numbers of expressed uORFs in their 5′ UTRs showed significantly lower translation efficiencies in both dark and L4h samples (Figure 5A; see Supplemental Figure 10A online). Thus, the association of ribosomes with uORFs could impose translation inhibition on their downstream mORFs. The inhibitory effects of uORFs on the translation of mORFs were more evident for L4h than dark samples (translation efficiency [TE] at L4h/dark; *D*-value = 1.9E-01, P value = 9.3E-08 for genes with at least three expressed uORFs; right panel in Figure 5A), perhaps to attenuate the light-enhanced translation in L4h observed previously (Liu et al., 2012).

Recent studies in both yeast and mammals suggested that the near-cognate codons, especially CTG, could also be translational initiation codons for uORFs (Ingolia et al., 2011; Brar et al., 2012; Fritsch et al., 2012; Lee et al., 2012). The identification of expressed uORFs starting with CTG in *Arabidopsis* indicated that this near-cognate initiation codon is also used by *Arabidopsis* uORFs (see Supplemental Figure 7 and Supplemental Data Set 2 online). Interestingly, TE was similar for mORFs on transcripts with CTG-mediated expressed uORFs and unexpressed uORFs in both dark and L4h samples (Figure 5B; see Supplemental Figure 10B online). Thus, only uORFs initiated with ATG but not CTG could negatively regulate the translation of the downstream mORFs in deetiolating *Arabidopsis*. Similarly, only ATG-mediated uORFs were found to act competitively on the translation of downstream mORFs in yeast (Brar et al., 2012).

Characterization of Downstream Translation Start Sites

In addition to identifying the expressed uORFs, the features of the RPFs predominantly mapped to translating regions also provides the possibility of revealing the alternative translational start sites downstream of annotated start sites. A higher read coverage at downstream ATGs other than the annotated ATG initiation codon may indicate an alternative translation start site. We identified 35 downstream ATGs in 31 genes (see Supplemental Figure 11 and Supplemental Data Set 3 online). Among them, *FARNESYL-DIPHOSPHATE SYNTHASE1* (*FPS1*) and *GLUTATHIONE S-TRANSFERASE PHI8* (*GSTF8*) were previously described to encode dual-targeting (cytosol and mitochondria) polypeptides (Cunillera

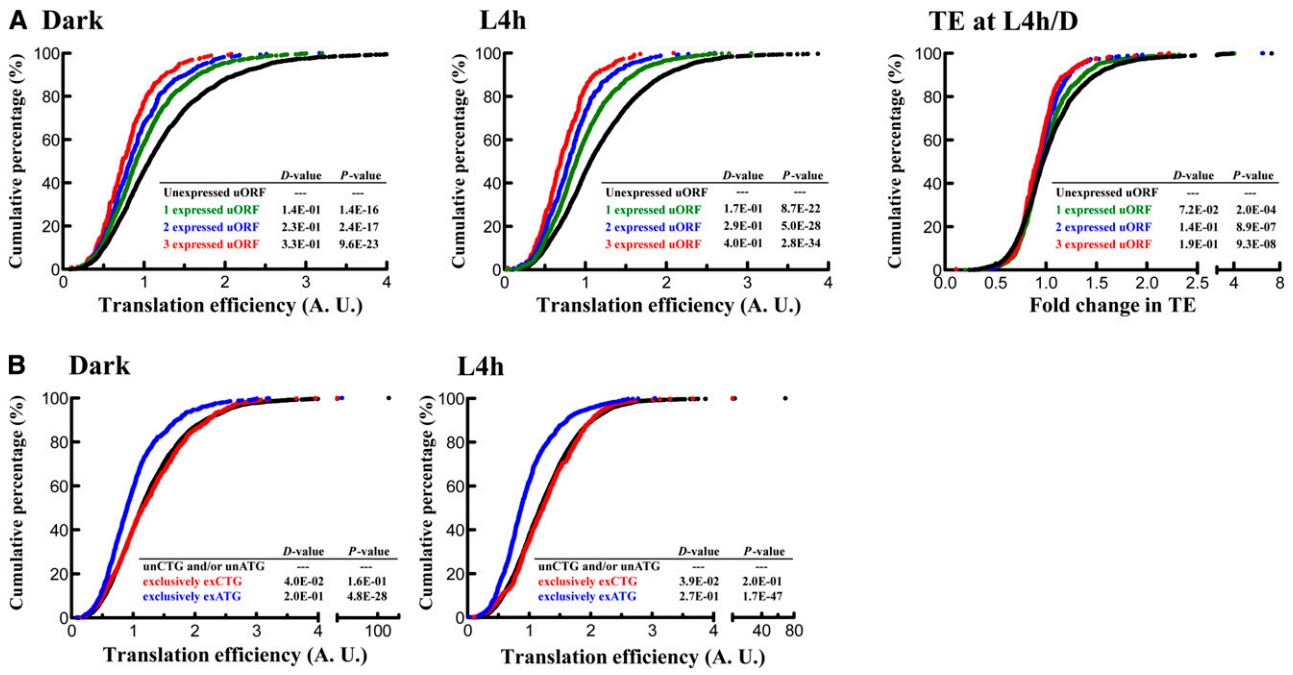

Figure 5. ATG-Initiated uORFs Repress the Translation of the Downstream mORF.

(A) Cumulative curves of the TE (in arbitrary units) of mORFs in transcripts without expressed uORFs or with 1, 2, or ≥3 expressed uORFs. Shown are fold changes in TE for dark and L4h samples for transcripts in four categories and *D*- and P values from the Kolmogorov-Smirnov test.
(B) Cumulative curves of TE (in arbitrary units [A.U.]) for mORFs in transcripts without expressed uORFs (unATG/unCTG), with expressed ATG (exATG) or expressed CTG (exCTG) initiated uORFs in their 5′ UTRs.

et al., 1997; Thatcher et al., 2007). In deetiolating *Arabidopsis*, FPS1 and GSTF8 were preferentially translated from the downstream ATGs for cytosolic forms (Figure 6A; see Supplemental Figure 12A and Supplemental Data Set 4 online). Our data further supported that a potential dual-targeting gene, *GLUTATHIONE PEROXIDASE6* (*GPX6*) (Rodriguez Milla et al., 2003), encoding the cytosolic isoform in deetiolating *Arabidopsis* (top panels in Figure 6B and Supplemental Figure 12B online; see Supplemental Data Set 4 online), and a transcription factor gene, *CONSTANS-LIKE4* (*COL4*) (bottom panels in Figure 6B and Supplemental Figure 12B online; see Supplemental Data Set 4 online), may produce a protein isoform with N-terminal truncation. Whether the choice of downstream ATGs was determined by alternative transcription sites or alternative transcript processing (Cunillera et al., 1997; Thatcher et al., 2007) remains to be clarified.

MiRNA Target Genes Have Lower Translational Efficiency

In plants, miRNAs can negatively regulate gene expression through miRNA-mediated mRNA cleavage and translation inhibition (Aukerman and Sakai, 2003; Chen, 2004; Gandikota et al., 2007; Brodersen et al., 2008; Lanet et al., 2009; Beauclair et al., 2010; Chen, 2010; Yang et al., 2012). However, the impact of miRNAs on translational repression has not been evaluated globally in *Arabidopsis*. To analyze this, we retrieved 1155 expressed genes as targets of 228 expressed miRNA from L4h data (transcripts per million >0; see Supplemental Figure 13 and

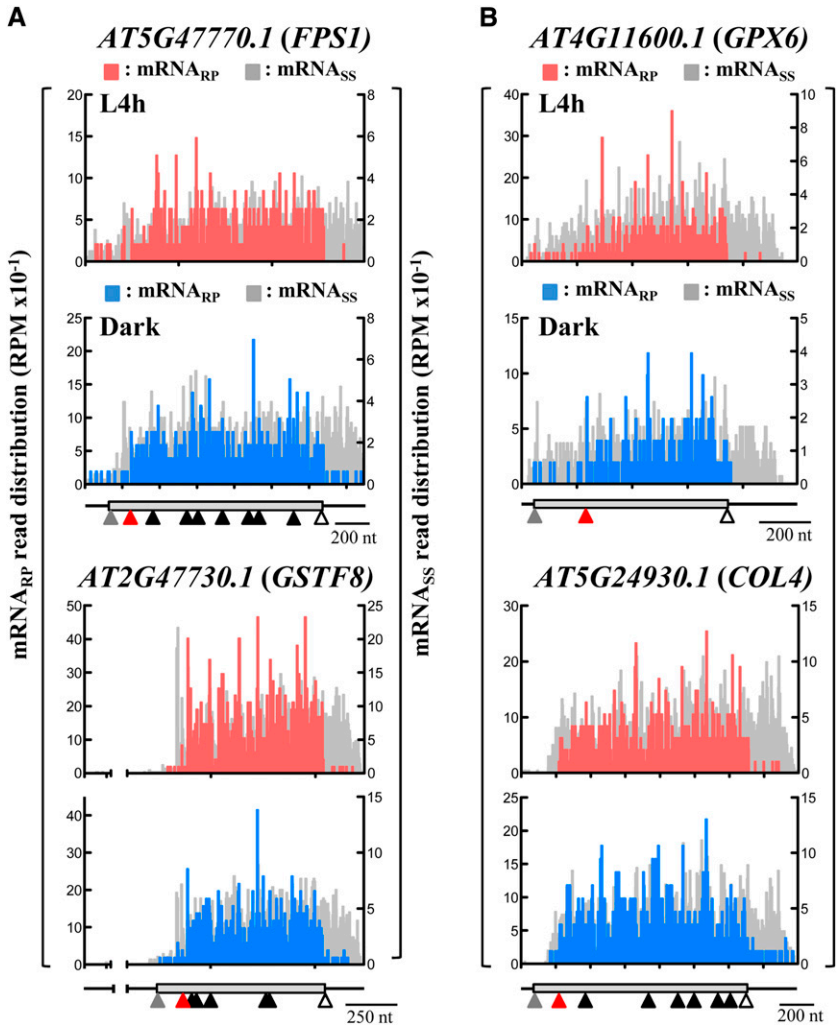

Figure 6. Representative Proteins with Alternative Translation Start Sites in Photomorphogenic *Arabidopsis*.

Read densities for mRNA$_{SS}$ and mRNA$_{RP}$ were plotted for *FARNESYL-DIPHOSPHATE SYNTHASE1* (*FPS1*) and *GLUTATHIONE S-TRANSFERASE PHI8* (*GSTF8*) **(A)** and *GLUTATHIONE PEROXIDASE6* (*GPX6*) and *CONSTANS-LIKE4* (*COL4*) **(B)**. For each gene, the annotated gene model is shown underneath the read distribution plot, with the UTR, CDS, annotated ATG, alternative ATG initiation sites, internal downstream ATGs, and stop codon marked with a black line, gray box, gray triangle, red triangle, filled black triangle, and open triangle, respectively. nt, nucleotides; RPM, reads per million.

Supplemental Data Set 5 online). We found that miRNA targets had significantly lower TE (Figure 7A; see Supplemental Figure 14A online). A similar conclusion was drawn for 971 expressed genes targeted by 203 expressed miRNAs in the dark (see Supplemental Figure 15A online). The $mRNA_{SS}$ density remained comparable for miRNA targets and nontargets (Figure 7B; see Supplemental Figures 14B and 15B online). However, the $mRNA_{RP}$ density was uniformly lower for miRNA targets than for nontargets spanning the CDS (Figure 7C; see Supplemental Figures 14C and 15C online), so miRNAs may exert their functions in inhibiting translation initiation or elongation, as was seen in *Drosophila melanogaster* and zebra fish (*Danio rerio*; Bazzini et al., 2012; Djuranovic et al., 2012).

Unlike the attenuating impact of uORFs on light-mediated translation enhancement (Figure 5A), light-regulated global changes in TE were comparable for miRNA targets and nontargets (see Supplemental Figure 15D online). Therefore, L4h treatment may affect the translation of only a subset of or specific miRNA target genes.

DISCUSSION

This study has expanded the current understanding of translation control in *Arabidopsis*. We identify additional light-responsive genes regulated at the translational level, provide molecular evidence for protein isoforms being translated, and show the differential influence of uORFs and miRNAs in the regulation of translation in photomorphogenic *Arabidopsis*.

Translating Ribosomes in Plants, Mammals, and Yeasts

Analogous to yeast and mammals (Ingolia et al., 2009; Guo et al., 2010; Ingolia et al., 2011), in *Arabidopsis*, we found that translating ribosomes were predominantly located in coding regions, protected ~30 nucleotides and moved in three-nucleotide periodicity (Figures 1 and 2; see Supplemental Figures 1 and 5A online), which suggests that these are conserved features across kingdoms.

The use of the 15th nucleotide of the RPFs in the mapping process revealed a clear offset between the UTR and the annotated initiation codon ATG (Figure 2A; see Supplemental Figure 4 online). This finding suggested the existence of a 14-nucleotide distance between the 5′ termini of protected fragments and the P-sites in *Arabidopsis* compared with the 12- or 13-nucleotide offset in yeast and mammals (Guo et al., 2010; Ingolia et al., 2011, 2012; Lee et al., 2012). The sizes of sequence fragments (27 to 30 nucleotides) in *Arabidopsis* are similar to those in yeast and mammals (Guo et al., 2010; Ingolia et al., 2011, 2012; Lee et al., 2012), which is unlikely to cause this slight offset. Alternatively, the differential composition of ribosomal proteins or rRNAs (18S/25S in *Arabidopsis*, 18S/26S in yeast, and 18S/28S in mammals) may contribute to different ribosome conformations, thus protecting mRNAs with slightly different sizes. Also, the magnesium concentration and ion strength in buffers used for *Arabidopsis* ribosome profiling could be optimized to further improve the nuclease digestion process, as was previously suggested (Ingolia et al., 2012). Nevertheless, this slight offset should not have affected the expression analyses used in this study.

Inhibitory Roles of Expressed uORFs on Translation of Downstream mORFs

Our genome-wide analyses provide systemic identification of the expressed uORFs in *Arabidopsis*. We also revealed inhibitory roles of ATG-initiated uORFs in the translation of downstream mORFs (Figure 5A; see Supplemental Figure 10A online). Because the expressed uORF(s) and the mORF are separate ORFs on a single transcript (see Supplemental Figure 7 online), a leaky scanning or reinitiation mechanism (Jackson et al., 2010) is needed for successful translation of the downstream mORF. A recent study in humans showed that the reinitiation process was less efficient than was leaking scanning (Lee et al., 2012), which is consistent with our results showing that transcripts with expressed uORFs have lower translational efficiency for mORFs. Also, this translational repression role of uORFs may be associated with their unique features (Figure 4; see Supplemental

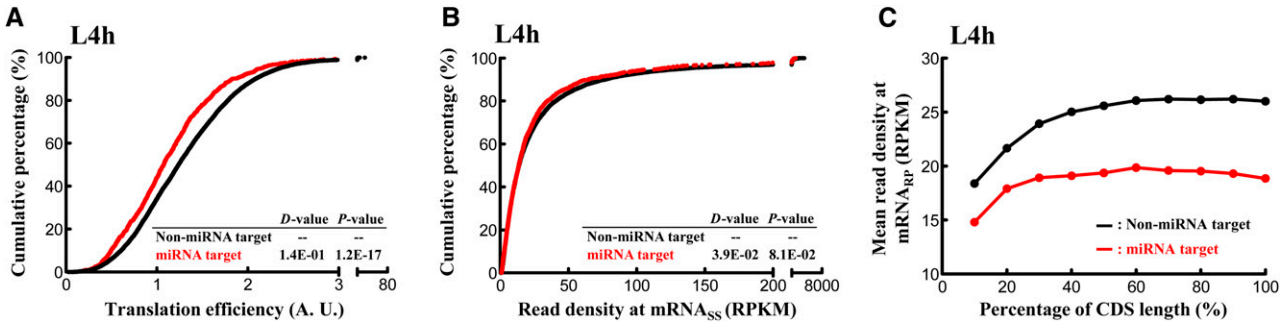

Figure 7. Widespread Low TE for MiRNA Target Genes in Photomorphogenic *Arabidopsis*.

(A) and **(B)** Cumulative curves of TE **(A)** or $mRNA_{SS}$ **(B)** for expressed *Arabidopsis* transcripts that are miRNA targets (in red, n = 1155) or nontargets (in black, n = 12,509) in L4h samples. Also shown are D- and P values from Kolmogorov-Smirnov tests. A.U., arbitrary units

(C) Mean $mRNA_{RP}$ densities against the CDS length for miRNA targets or nontargets in L4h samples. The full-length CDS were divided into 10 bins for each expressed transcript. Read densities for genes with expression in the 10th to 90th percentiles were used for calculating the mean $mRNA_{RP}$ density to avoid skewing the data by extreme values.

Figure 9 online). The longer uORFs may occupy and/or compete for the translation initiation factors. Also, the shorter distance between expressed uORFs and mORFs may hinder the scanning 40S ribosome for recruiting a new initiation complex (Kozak, 1987b, 2001; Rajkowitsch et al., 2004; Roy et al., 2010).

Codon usage affects the moving speed of translating ribosomes (Varenne et al., 1984; Shu et al., 2006). A rare Leu codon in uORF1 led to the formation of a ribosome block for translation inhibition of the downstream mORF for *Xenopus laevis* Connexin41 mRNA (Meijer and Thomas, 2003). In our analyses (Figure 4C; see Supplemental Figure 9C online), expressed uORFs did not prefer rare codons, which suggests that the inhibitory role of uORFs is not due to the stalling of ribosomes at 5′ UTRs.

Previous studies also provided evidence that the uORF-encoded peptides in yeast CPA1 and the *Neurospora crassa arg-2* transcripts could negatively regulate translation by triggering mRNA decay (reviewed in Hood et al., 2009). For *msl-2* mRNA in *Drosophila*, the uORF works in conjunction with a second *cis*-element and a *trans*-acting RNA binding protein Sex-lethal to inhibit its downstream mORF (Medenbach et al., 2011). The identification of translating uORFs offers promising opportunities to examine the diverse action mechanisms of uORFs in the translation of annotated mORFs.

Global Translational Repression of MiRNA Target Transcripts

Our results showed that miRNA target transcripts have significantly lower translational efficiency, likely because of the even decrease in ribosome density on the CDS (Figure 7; see Supplemental Figures 14 and 15 online). A recent report also demonstrated a predominant translation repression mediated by miRNAs in multiple plant species (Li et al., 2013a). The translation inhibition likely occurs on the endoplasmic reticulum in *Arabidopsis* (Li et al., 2013b).

The association of miRNAs or an RNA-induced silencing complex and target transcripts undergoing translation may result in a "traffic jam" of ribosomes that would appear as a stalling of ribosomes, possibly at the 5′ end of miRNA target sites. We did not observe such ribosome-stalling sites upstream of putative miRNA target sites, which is consistent with the lack of ribosome pausing in heterochronic miRNA target transcripts in *Caenorhabditis elegans* (Stadler et al., 2012).

MiRNAs were found to act first on mRNA translation, then decapping or decay of mRNAs (Bazzini et al., 2012; Djuranovic et al., 2012). A recent study concluded that miRNA targeting at the CDS leads to translational inhibition, whereas targeting at the 3′ UTR preferentially results in mRNA degradation (Hausser et al., 2013). In our study, despite the clear decrease in $mRNA_{RP}$ level for miRNA targets (Figure 7C; see Supplemental Figures 14C and 15C online), $mRNA_{SS}$ levels did not differ between miRNA targets and nontargets (Figure 7B; see Supplemental Figures 14B and 15B online), which is consistent with the predominant presence of miRNA target sites in CDS regions (77%). In plants, miRNA-mediated cleavage of target transcripts account for many of the miRNA-triggered gene-silencing events reported previously. By adopting a stringent expression threshold in defining expressed miRNA target genes in our analyses (see Supplemental Figure 13 online), we may have eliminated genes with low expression resulting from miRNA-mediated decay. Nevertheless, our study clearly highlights a global effect of miRNA-mediated translational repression via reduced ribosome occupancy for most miRNA targets.

METHODS

Preparation of Ribosome-Protected and Randomly Fragmented mRNAs

Arabidopsis thaliana ecotype Columbia-0 plants were grown and treated (dark or L4h) as described previously (Liu et al., 2012). By pouring liquid N_2 directly into Petri dishes, aerial parts of seedlings were harvested, frozen, and stored at −80°C. The *Arabidopsis* polysome complexes were extracted with polysome extraction buffer (200 mM Tris-HCl, pH 8, 50 mM KCl, 25 mM $MgCl_2$, 100 μg/mL cycloheximide, 2% polyoxyethylene 10 tridecyl ether, 1% deoxycholic acid, and 1 mM DTT). The digestion and purification of RPFs were as described (Ingolia et al., 2011), except that 14 mL of polysome extract was digested with RNase I (10 units/μg RNA; New England Biolabs) at room temperature for 1 h. The reaction was stopped by adding Superase In (4 units/μg RNA; Ambion) and immediately loaded on a 1 M Suc cushion containing 0.1 units/μL Superase In for pelleting the ribosomes. The SDS/phenol method was used to purify the RPFs.

Total RNA isolated as described previously (Chang et al., 2008) was used for total mRNA purification with the Illustra mRNA purification kit (GE Healthcare). The mRNA was fragmented with NEBNext RNA fragmentation reaction buffer (NEB) at 94°C for 40 min.

cDNA Library Construction and Deep Sequencing

Ribosome-protected or random mRNA fragments were used to construct libraries as described (Ingolia et al., 2011) with the RT primer sequence 5′-(P)GATCGTCGGACTGTAGAACTCTGAACGTGTAGATC(Sp18)CACTCA(Sp18)CAAGCAGAAGACGGCATACGATCCAATTGATGGTGCCTACAG-3′ (Sp18 is an 18-atom hexa-ethyleneglycol spacer). Amplification of cDNA involved use of 0.5 units of Phusion polymerase (NEB) with 30-s denaturation at 98°C, then eight cycles of 10-s denaturation at 98°C, 10-s annealing at 60°C, and 5-s extension at 72°C. Deep sequencing involved use of Illumina HiSeq2000 at Yourgene Bio Science (Taipei). For $mRNA_{SS}$ reads, dark and L4h samples were separately indexed and sequenced in the same lane. For $mRNA_{RP}$ reads, dark and L4h samples were each sequenced in one lane.

Sequencing Data Mapping and Analyses

Reference transcript data sets including the 5′ UTRs, CDS, and 3′ UTRs for 27,416 annotated protein-coding gene models were retrieved from The Arabidopsis Information Resources database (TAIR10; http://www.Arabidopsis.org). Among them, 8572 protein-coding genes lacked annotated UTRs (see Supplemental Figure 16 online). We have updated gene models of some genes lacking 5′/3′ UTRs using our sequencing data sets outlined in Supplemental Figure 16 online. The updated gene models are referred to as the extended protein-coding gene models in this study. For mapping reads to the transcripts of the extended protein-coding gene models, raw reads were processed and mapped as described in Supplemental Figure 2 online. Only unique mapped reads were aligned and included for calculating the read density of each gene. The 15th nucleotide of aligned reads was used for calculating the read count of each individual transcript. *AT2G01021.1* was removed from the reference transcript data set because its sequence perfectly matched the *Arabidopsis* rRNA gene (GenBank: X52320.1) and had a large read count

in our $mRNA_{RP}$ data. The filtering processes and criteria used for identifying translationally regulated genes, position-based read densities, ATG- or CTG-initiated uORFs, the downstream in-frame ATG initiation codon, and miRNA target genes are outlined in Supplemental Figures 2, 7, 11, and 13 online. The usage frequency for each *Arabidopsis* codon (Figure 4C and see Supplemental Figure 9 online) was from a previous report (Nakamura et al., 2000). As a control for data shown in Supplemental Figure 5C online, the CDSs for each protein coding gene were randomly shuffled by the shuffle function in perl, and the codon usages were calculated as described (Tuller et al., 2010). The TE of mORFs and uORFs (Figures 3, 5, and 7 and see Supplemental Figures 6, 10, 14, and 15 online) was computed by normalizing the densities of $mRNA_{RP}$ for mORFs or uORFs to those of $mRNA_{SS}$ for the whole transcript.

RNA Gel Blot Analysis

Total polysomal RNAs treated with or without RNase I from dark or L4h samples were separated on 15% denaturing polyacrylamide Tris-borate ethylenediaminetetraacetic acid-Urea gel (Invitrogen) and transferred to nylon membrane (Hybond N^+; Amersham GE Healthcare) using a transblot semidry transfer cell (Bio-Rad). A 992-bp DNA fragment of *AT2G45960* was amplified with the primer sequences 5′-ACATAACCCACTCACA-GAAAAACC-3′ and 5′-CACAGGTAGTAGATTCACAAAAGA-3′ in the presence of Digoxigenin-11-dUTP alkali-labile (Roche). The hybridization and signal detection were as suggested in the DIG System User's Guide (Roche), except that the hybridization was performed with FastHyb-Hybridization Solution (BioChain) at 37°C for overnight.

Sequencing of Small RNAs

Arabidopsis ecotype Columbia-0 plants were grown, treated (dark or 3-h light), and harvested as described above. Total RNA was isolated with use of the mirVana miRNA isolation kit (Invitrogen). The size-fractionated small RNAs were used to generate libraries for sequencing by the Illumina platform. Mapping of the sequencing reads to known miRNAs resulted in 203 (dark) and 228 (3-h light) expressed miRNAs (transcripts per million > 0) used in this study.

Gene Ontology Analyses

The enriched functional groups were revealed with use of the elim method from the TopGO package (Alexa et al., 2006) implemented in the MultiView plugin of GOBU (Lin et al., 2006). The Fisher exact test was used to evaluate the representation differences between genes in the light-up-regulated group and those not upregulated by light in the whole genome. Only GO terms with preferential representation in the category of biological process (P value < 1E-05) from the light-upregulated group were selected.

Statistical Analyses

The Kolmogorov-Smirnov test downloaded from the Arizona Laserchron Center at the University of Arizona (https://docs.google.com/View?id=dcbpr8b2_7c3s6pxft) was used for calculating *D*- and P values with the no error option. One-tailed Fisher's exact test was performed online (http://www.matforsk.no/ola/fisher.htm). Z-scores were calculated by the Standardize formula in Microsoft Excel.

Accession Numbers

Sequencing data from this article can be found in the National Center for Biotechnology Information's Gene Expression Omnibus under accession number GSE43703. Names and locus numbers for genes described in this study are listed in Figures 3 and 6, Supplemental Figures 6 and 12 online, and Supplemental Data Sets 1 to 5 online.

Supplemental Data

The following materials are available in the online version of this article.

Supplemental Figure 1. RNA Gel Blot Analysis of Ribosome-Protected mRNA Fragments in *Arabidopsis*.

Supplemental Figure 2. A Flowchart and Summary of the Read Mapping.

Supplemental Figure 3. Two Biological Replicates Provide Comparable Data Resolution.

Supplemental Figure 4. $mRNA_{RP}$ Reads Are Enriched in CDS (Rep 2).

Supplemental Figure 5. Positional Analyses of $mRNA_{SS}$ and $mRNA_{RP}$ in CDS Regions.

Supplemental Figure 6. Ribosome Profiling Identifies Additional Genes Regulated at the Translational Level in Photomorphogenic *Arabidopsis* (Rep 2).

Supplemental Figure 7. A Flowchart of the Data Analysis Procedure for Identifying and Categorizing ATG- or CTG-Initiated uORFs.

Supplemental Figure 8. Expressed uORFs Are Active Translating Units.

Supplemental Figure 9. Sequence Characteristics of Expressed Upstream Open Reading Frames in *Arabidopsis* Transcripts (Rep 2).

Supplemental Figure 10. ATG-Initiated uORFs Repress the Translation of the Downstream mORF (Rep 2).

Supplemental Figure 11. A Flowchart of the Procedure for Identifying Downstream in-Frame Translation Start Codons.

Supplemental Figure 12. Representative Proteins with Alternative Translation Start Sites in Photomorphogenic *Arabidopsis* (Rep 2).

Supplemental Figure 13. A Flowchart of the Procedure for Identifying MiRNA Target Genes.

Supplemental Figure 14. Widespread Low Translation Efficiency for MiRNA Target Genes in Photomorphogenic *Arabidopsis* (Rep 2).

Supplemental Figure 15. Widespread Lower Translation Efficiency for MiRNA Target Genes in Etiolated *Arabidopsis*.

Supplemental Data Set 1. List of Genes Up- (z-score >2) or Down-regulated (z-score <−2) by Light at the Translational Level.

Supplemental Data Set 2. List of Expressed Genes with One or More uORFs.

Supplemental Data Set 3. List of 31 Genes with 35 in-Frame dATGs.

Supplemental Data Set 4. dATGs for Representative Loci in Figure 6 and Supplemental Figure 12.

Supplemental Data Set 5. Lists of the 971 and 1155 Genes Predicted to Be Targets of Expressed MiRNA(s) under Dark and L4h Conditions, Respectively.

ACKNOWLEDGMENTS

This research was supported by a research grant and Investigator Award (to Sh.-H.W.) from Academia Sinica and a fellowship (to Sz.-H.W.) from the Taiwan International Graduate Program.

AUTHOR CONTRIBUTIONS

M.-J.L., Sz.-H.W., and Sh.-H.W. designed the research. Sz.-H.W., J.-F.W., Y.-C.W., and H.-L.T. performed experiments. M.-J.L., W.-D.L., T.-Y.T., and Sh.-H.W. analyzed the data. M.-J.L. and Sh.-H.W. wrote the article.

Received June 11, 2013; revised September 27, 2013; accepted October 11, 2013; published October 31, 2013.

REFERENCES

Alatorre-Cobos, F., Cruz-Ramírez, A., Hayden, C.A., Pérez-Torres, C.A., Chauvin, A.L., Ibarra-Laclette, E., Alva-Cortés, E., Jorgensen, R.A., and Herrera-Estrella, L. (2012). Translational regulation of *Arabidopsis* XIPOTL1 is modulated by phosphocholine levels via the phylogenetically conserved upstream open reading frame 30. J. Exp. Bot. **63:** 5203–5221.

Alexa, A., Rahnenführer, J., and Lengauer, T. (2006). Improved scoring of functional groups from gene expression data by decorrelating GO graph structure. Bioinformatics **22:** 1600–1607.

Arava, Y., Wang, Y., Storey, J.D., Liu, C.L., Brown, P.O., and Herschlag, D. (2003). Genome-wide analysis of mRNA translation profiles in *Saccharomyces cerevisiae*. Proc. Natl. Acad. Sci. USA **100:** 3889–3894.

Aukerman, M.J., and Sakai, H. (2003). Regulation of flowering time and floral organ identity by a microRNA and its APETALA2-like target genes. Plant Cell **15:** 2730–2741.

Bazzini, A.A., Lee, M.T., and Giraldez, A.J. (2012). Ribosome profiling shows that miR-430 reduces translation before causing mRNA decay in zebrafish. Science **336:** 233–237.

Beauclair, L., Yu, A., and Bouché, N. (2010). MicroRNA-directed cleavage and translational repression of the copper chaperone for superoxide dismutase mRNA in *Arabidopsis*. Plant J. **62:** 454–462.

Branco-Price, C., Kaiser, K.A., Jang, C.J., Larive, C.K., and Bailey-Serres, J. (2008). Selective mRNA translation coordinates energetic and metabolic adjustments to cellular oxygen deprivation and reoxygenation in *Arabidopsis thaliana*. Plant J. **56:** 743–755.

Branco-Price, C., Kawaguchi, R., Ferreira, R.B., and Bailey-Serres, J. (2005). Genome-wide analysis of transcript abundance and translation in *Arabidopsis* seedlings subjected to oxygen deprivation. Ann. Bot. (Lond.) **96:** 647–660.

Brar, G.A., Yassour, M., Friedman, N., Regev, A., Ingolia, N.T., and Weissman, J.S. (2012). High-resolution view of the yeast meiotic program revealed by ribosome profiling. Science **335:** 552–557.

Brodersen, P., Sakvarelidze-Achard, L., Bruun-Rasmussen, M., Dunoyer, P., Yamamoto, Y.Y., Sieburth, L., and Voinnet, O. (2008). Widespread translational inhibition by plant miRNAs and siRNAs. Science **320:** 1185–1190.

Chang, C.S., Li, Y.H., Chen, L.T., Chen, W.C., Hsieh, W.P., Shin, J., Jane, W.N., Chou, S.J., Choi, G., Hu, J.M., Somerville, S., and Wu, S.H. (2008). LZF1, a HY5-regulated transcriptional factor, functions in *Arabidopsis* de-etiolation. Plant J. **54:** 205–219.

Chen, X. (2004). A microRNA as a translational repressor of APETALA2 in *Arabidopsis* flower development. Science **303:** 2022–2025.

Chen, X. (2010). Small RNAs - Secrets and surprises of the genome. Plant J. **61:** 941–958.

Cunillera, N., Boronat, A., and Ferrer, A. (1997). The *Arabidopsis thaliana* FPS1 gene generates a novel mRNA that encodes a mitochondrial farnesyl-diphosphate synthase isoform. J. Biol. Chem. **272:** 15381–15388.

Djuranovic, S., Nahvi, A., and Green, R. (2012). MiRNA-mediated gene silencing by translational repression followed by mRNA deadenylation and decay. Science **336:** 237–240.

Fabian, M.R., Sonenberg, N., and Filipowicz, W. (2010). Regulation of mRNA translation and stability by microRNAs. Annu. Rev. Biochem. **79:** 351–379.

Fritsch, C., Herrmann, A., Nothnagel, M., Szafranski, K., Huse, K., Schumann, F., Schreiber, S., Platzer, M., Krawczak, M., Hampe, J., and Brosch, M. (2012). Genome-wide search for novel human uORFs and N-terminal protein extensions using ribosomal footprinting. Genome Res. **22:** 2208–2218.

Gandikota, M., Birkenbihl, R.P., Höhmann, S., Cardon, G.H., Saedler, H., and Huijser, P. (2007). The miRNA156/157 recognition element in the 3′ UTR of the *Arabidopsis* SBP box gene SPL3 prevents early flowering by translational inhibition in seedlings. Plant J. **49:** 683–693.

Guo, H., Ingolia, N.T., Weissman, J.S., and Bartel, D.P. (2010). Mammalian microRNAs predominantly act to decrease target mRNA levels. Nature **466:** 835–840.

Hanfrey, C., Franceschetti, M., Mayer, M.J., Illingworth, C., and Michael, A.J. (2002). Abrogation of upstream open reading frame-mediated translational control of a plant S-adenosylmethionine decarboxylase results in polyamine disruption and growth perturbations. J. Biol. Chem. **277:** 44131–44139.

Hausser, J., Syed, A.P., Bilen, B., and Zavolan, M. (2013). Analysis of CDS-located miRNA target sites suggests that they can effectively inhibit translation. Genome Res. **23:** 604–615.

\Hayden, C.A., and Jorgensen, R.A. (2007). Identification of novel conserved peptide uORF homology groups in *Arabidopsis* and rice reveals ancient eukaryotic origin of select groups and preferential association with transcription factor-encoding genes. BMC Biol. **5:** 32.

Hood, H.M., Neafsey, D.E., Galagan, J., and Sachs, M.S. (2009). Evolutionary roles of upstream open reading frames in mediating gene regulation in fungi. Annu. Rev. Microbiol. **63:** 385–409.

Huntzinger, E., and Izaurralde, E. (2011). Gene silencing by microRNAs: Contributions of translational repression and mRNA decay. Nat. Rev. Genet. **12:** 99–110.

Imai, A., Hanzawa, Y., Komura, M., Yamamoto, K.T., Komeda, Y., and Takahashi, T. (2006). The dwarf phenotype of the *Arabidopsis* acl5 mutant is suppressed by a mutation in an upstream ORF of a bHLH gene. Development **133:** 3575–3585.

Ingolia, N.T., Brar, G.A., Rouskin, S., McGeachy, A.M., and Weissman, J.S. (2012). The ribosome profiling strategy for monitoring translation in vivo by deep sequencing of ribosome-protected mRNA fragments. Nat. Protoc. **7:** 1534–1550.

Ingolia, N.T., Ghaemmaghami, S., Newman, J.R., and Weissman, J.S. (2009). Genome-wide analysis in vivo of translation with nucleotide resolution using ribosome profiling. Science **324:** 218–223.

Ingolia, N.T., Lareau, L.F., and Weissman, J.S. (2011). Ribosome profiling of mouse embryonic stem cells reveals the complexity and dynamics of mammalian proteomes. Cell **147:** 789–802.

Jackson, R.J., Hellen, C.U., and Pestova, T.V. (2010). The mechanism of eukaryotic translation initiation and principles of its regulation. Nat. Rev. Mol. Cell Biol. **11:** 113–127.

Juntawong, P., and Bailey-Serres, J. (2012). Dynamic light regulation of translation status in *Arabidopsis thaliana*. Front Plant Sci **3:** 66.

Kawaguchi, R., Girke, T., Bray, E.A., and Bailey-Serres, J. (2004). Differential mRNA translation contributes to gene regulation under non-stress and dehydration stress conditions in *Arabidopsis thaliana*. Plant J. **38:** 823–839.

Kim, B.H., Cai, X., Vaughn, J.N., and von Arnim, A.G. (2007). On the functions of the h subunit of eukaryotic initiation factor 3 in late stages of translation initiation. Genome Biol. **8:** R60.

Kozak, M. (1986). Point mutations define a sequence flanking the AUG initiator codon that modulates translation by eukaryotic ribosomes. Cell **44:** 283–292.

Kozak, M. (1987a). An analysis of 5′-noncoding sequences from 699 vertebrate messenger RNAs. Nucleic Acids Res. **15:** 8125–8148.

Kozak, M. (1987b). Effects of intercistronic length on the efficiency of reinitiation by eucaryotic ribosomes. Mol. Cell. Biol. **7:** 3438–3445.

Kozak, M. (2001). Constraints on reinitiation of translation in mammals. Nucleic Acids Res. **29:** 5226–5232.

Lackner, D.H., and Bähler, J. (2008). Translational control of gene expression from transcripts to transcriptomes. Int. Rev. Cell Mol. Biol. **271:** 199–251.

Lanet, E., Delannoy, E., Sormani, R., Floris, M., Brodersen, P., Crété, P., Voinnet, O., and Robaglia, C. (2009). Biochemical evidence for translational repression by *Arabidopsis* microRNAs. Plant Cell **21:** 1762–1768.

Lee, S., Liu, B., Lee, S., Huang, S.X., Shen, B., and Qian, S.B. (2012). Global mapping of translation initiation sites in mammalian cells at single-nucleotide resolution. Proc. Natl. Acad. Sci. USA **109:** E2424–E2432.

Li, J.F., Chung, H.S., Niu, Y., Bush, J., McCormack, M., and Sheen, J. (2013a). Comprehensive protein-based artificial microRNA screens for effective gene silencing in plants. Plant Cell **25:** 1507–1522.

Li, S., et al. (2013b). MicroRNAs inhibit the translation of target mRNAs on the endoplasmic reticulum in *Arabidopsis*. Cell **153:** 562–574.

Lin, W.D., Chen, Y.C., Ho, J.M., and Hsiao, C.D. (2006). GOBU: Toward an integration interface for biological objects. J. Inf. Sci. Eng. **22:** 19–29.

Liu, M.J., Wu, S.H., Chen, H.M., and Wu, S.H. (2012). Widespread translational control contributes to the regulation of *Arabidopsis* photomorphogenesis. Mol. Syst. Biol. **8:** 566.

Mackenzie, S.A. (2005). Plant organellar protein targeting: A traffic plan still under construction. Trends Cell Biol. **15:** 548–554.

Matsuura, H., Ishibashi, Y., Shinmyo, A., Kanaya, S., and Kato, K. (2010). Genome-wide analyses of early translational responses to elevated temperature and high salinity in *Arabidopsis thaliana*. Plant Cell Physiol. **51:** 448–462.

Medenbach, J., Seiler, M., and Hentze, M.W. (2011). Translational control via protein-regulated upstream open reading frames. Cell **145:** 902–913.

Meijer, H.A., and Thomas, A.A. (2003). Ribosomes stalling on uORF1 in the Xenopus Cx41 5′ UTR inhibit downstream translation initiation. Nucleic Acids Res. **31:** 3174–3184.

Melamed, D., and Arava, Y. (2007). Genome-wide analysis of mRNA polysomal profiles with spotted DNA microarrays. Methods Enzymol. **431:** 177–201.

Morris, D.R., and Geballe, A.P. (2000). Upstream open reading frames as regulators of mRNA translation. Mol. Cell. Biol. **20:** 8635–8642.

Mustroph, A., Juntawong, P., and Bailey-Serres, J. (2009). Isolation of plant polysomal mRNA by differential centrifugation and ribosome immunopurification methods. Methods Mol. Biol. **553:** 109–126.

Nakamura, Y., Gojobori, T., and Ikemura, T. (2000). Codon usage tabulated from international DNA sequence databases: status for the year 2000. Nucleic Acids Res. **28:** 292.

Nicolaï, M., Roncato, M.A., Canoy, A.S., Rouquié, D., Sarda, X., Freyssinet, G., and Robaglia, C. (2006). Large-scale analysis of mRNA translation states during sucrose starvation in Arabidopsis cells identifies cell proliferation and chromatin structure as targets of translational control. Plant Physiol. **141:** 663–673.

Nishimura, T., Wada, T., Yamamoto, K.T., and Okada, K. (2005). The *Arabidopsis* STV1 protein, responsible for translation reinitiation, is required for auxin-mediated gynoecium patterning. Plant Cell **17:** 2940–2953.

Pesole, G., Gissi, C., Grillo, G., Licciulli, F., Liuni, S., and Saccone, C. (2000). Analysis of oligonucleotide AUG start codon context in eukariotic mRNAs. Gene **261:** 85–91.

Piques, M., Schulze, W.X., Höhne, M., Usadel, B., Gibon, Y., Rohwer, J., and Stitt, M. (2009). Ribosome and transcript copy numbers, polysome occupancy and enzyme dynamics in *Arabidopsis*. Mol. Syst. Biol. **5:** 314.

Rajkowitsch, L., Vilela, C., Berthelot, K., Ramirez, C.V., and McCarthy, J.E. (2004). Reinitiation and recycling are distinct processes occurring downstream of translation termination in yeast. J. Mol. Biol. **335:** 71–85.

Ribeiro, D.M., Araújo, W.L., Fernie, A.R., Schippers, J.H., and Mueller-Roeber, B. (2012). Translatome and metabolome effects triggered by gibberellins during rosette growth in *Arabidopsis*. J. Exp. Bot. **63:** 2769–2786.

Rodriguez Milla, M.A., Maurer, A., Rodriguez Huete, A., and Gustafson, J.P. (2003). Glutathione peroxidase genes in *Arabidopsis* are ubiquitous and regulated by abiotic stresses through diverse signaling pathways. Plant J. **36:** 602–615.

Rosado, A., Li, R., van de Ven, W., Hsu, E., and Raikhel, N.V. (2012). *Arabidopsis* ribosomal proteins control developmental programs through translational regulation of auxin response factors. Proc. Natl. Acad. Sci. USA **109:** 19537–19544.

Roy, B., Vaughn, J.N., Kim, B.H., Zhou, F., Gilchrist, M.A., and Von Arnim, A.G. (2010). The h subunit of eIF3 promotes reinitiation competence during translation of mRNAs harboring upstream open reading frames. RNA **16:** 748–761.

Shu, P., Dai, H., Gao, W., and Goldman, E. (2006). Inhibition of translation by consecutive rare leucine codons in *E. coli*: Absence of effect of varying mRNA stability. Gene Expr. **13:** 97–106.

Sormani, R., Delannoy, E., Lageix, S., Bitton, F., Lanet, E., Saez-Vasquez, J., Deragon, J.M., Renou, J.P., and Robaglia, C. (2011). Sublethal cadmium intoxication in *Arabidopsis thaliana* impacts translation at multiple levels. Plant Cell Physiol. **52:** 436–447.

Stadler, M., Artiles, K., Pak, J., and Fire, A. (2012). Contributions of mRNA abundance, ribosome loading, and post- or peri-translational effects to temporal repression of *C. elegans* heterochronic miRNA targets. Genome Res. **22:** 2418–2426.

Thatcher, L.F., Carrie, C., Andersson, C.R., Sivasithamparam, K., Whelan, J., and Singh, K.B. (2007). Differential gene expression and subcellular targeting of *Arabidopsis* glutathione S-transferase F8 is achieved through alternative transcription start sites. J. Biol. Chem. **282:** 28915–28928.

Tuller, T., Carmi, A., Vestsigian, K., Navon, S., Dorfan, Y., Zaborske, J., Pan, T., Dahan, O., Furman, I., and Pilpel, Y. (2010). An evolutionarily conserved mechanism for controlling the efficiency of protein translation. Cell **141:** 344–354.

Varenne, S., Buc, J., Lloubes, R., and Lazdunski, C. (1984). Translation is a non-uniform process. Effect of tRNA availability on the rate of elongation of nascent polypeptide chains. J. Mol. Biol. **180:** 549–576.

Wiese, A., Elzinga, N., Wobbes, B., and Smeekens, S. (2004). A conserved upstream open reading frame mediates sucrose-induced repression of translation. Plant Cell **16:** 1717–1729.

Yang, L., Wu, G., and Poethig, R.S. (2012). Mutations in the GW-repeat protein SUO reveal a developmental function for microRNA-mediated translational repression in *Arabidopsis*. Proc. Natl. Acad. Sci. USA **109:** 315–320.